Single-Mode Helical Sapphire Bragg Grating for High-Temperature Sensing

Xizhen Xu , Jia He, Jiafeng Wu , Runxiao Chen, Fan Zhou, Benzhang Wang, Yupeng Zhang,
Yiping Wang , *Senior Member, IEEE, Fellow, OSA*, and Jun He , *Member, IEEE*

Abstract—Sapphire fiber Bragg grating (SFBG) is a potential high-temperature sensor, which can withstand 1900 °C. However, the broadband reflection spectrum of SFBG results from the multi-mode operation, hampering the sensing performance significantly. In this paper, we have reported on a single-mode SFBG based on the helical structure created by using a femtosecond laser direct writing technique. We found that the ring-shaped inscription pattern inscribed in sapphire fiber is irregular due to the focal-point distortion induced by the cylindrical geometry of the sapphire fiber. A slit beam shaping method was employed to solve this problem. By using the optimized slit width of 0.35 mm, the regular ring patterns can be inscribed within the sapphire fiber successfully. Such a structure has the maximum negative refractive index change of -8.8×10^{-3} and a width of 7.7 μm, which can serve as depressed cladding waveguide. Moreover, helical structures with various diameters have been created in sapphire fibers. The near-field profiles of the transmission mode and the spectra have been measured. The experimental results show that a single-mode helical SFBG with a diameter of 14 μm and a period of 1.78 μm can be achieved, exhibiting a narrow bandwidth of 0.18 nm and a high reflectivity

of 66.3%. In addition, the temperature sensing performance of a single-mode SFBG was studied. Such a device shows increasing temperature sensitivity at elevated temperatures, i.e., 22.5 pm/°C at 20 °C, 27.5 pm/°C at 600 °C and 33.9 pm/°C at 1200 °C, which is similar to the conventional multimode SFBG. However, its temperature response has much better repeatability than that of the multimode SFBG, benefiting from the single-mode transmission with high stability. Hence, the proposed single-mode SFBG is a promising high-temperature sensor, that can be applied in many fields, for example, power plants, gas turbines, and hypersonic vehicles.

I. INTRODUCTION

HIGH-TEMPERATURE measurement is important in various application fields, such as metallurgy, aviation, and gas-fired boilers. For example, the gas turbine is a key equipment in aviation and ships. Its performance depends on the turbine inlet temperature. The efficiency and power output of a gas turbine engine can be significantly enhanced by increasing its operating temperature [1], such as, the turbine inlet temperature of the F119 engine being more than 1700 °C [2]. Turbine blades are the components of an engine, which are subjected to ultra-high temperature environments. To improve the engine performance and value the life design, the safety and reliability of these turbine blades need to be investigated. Hence, temperature, the most intuitive indicator, should be detected in situ, which can reflect the working state of the turbine blades. Femtosecond-laser-inscribed fiber Bragg gratings (FBGs) are potential candidates, owing to high thermal resistance, compact size, and capability of multiplexing, which are more attractive for high-temperature sensing. However, silica-based FBGs can only operate at 1000 °C for a short time, limited by the glass-transition temperature (i.e., 1330 °C) [3]. In extreme cases, regenerated FBG fabricated in special Er-YZCAPS-fibers can withstand temperatures of up to 1400 °C [4].

Single-crystal sapphire fibers with an ultrahigh smelting point (2050 °C) are used to create FBGs, which can operate at extremely high temperatures of up to 1900 °C [5], [6], [7]. It has the ability to transmit a broad range of light wavelengths from 150 to 6000 nm and the attenuation is as small as 0.5~1.0 dB/m in near IR, which indicating that sapphire fiber is a promising material for high-temperature measurement. However, compared with standard fiber, single-crystal sapphire fiber cannot be grown in

Xizhen Xu, Yiping Wang, and Jun He are with the State Key Laboratory of Radio Frequency Heterogeneous Integration, Key Laboratory of Optoelectronic Devices and Systems of Ministry of Education/Guangdong Province, College of Physics and Optoelectronic Engineering, Shenzhen University, Shenzhen 518060, China, also with the Shenzhen Key Laboratory of Ultrafast Laser Micro/Nano Manufacturing, Guangdong and Hong Kong Joint Research Centre for Optical Fibre Sensors, Shenzhen University, Shenzhen 518060, China, and also with the Guangdong Laboratory of Artificial Intelligence and Digital Economy (SZ), Shenzhen 518107, China (e-mail: xizhenxu@szu.edu.cn; ypwang@szu.edu.cn; hejun07@szu.edu.cn).

Jia He, Jiafeng Wu, and Runxiao Chen are with the State Key Laboratory of Radio Frequency Heterogeneous Integration, Key Laboratory of Optoelectronic Devices and Systems of Ministry of Education/Guangdong Province, College of Physics and Optoelectronic Engineering, Shenzhen University, Shenzhen 518060, China, and also with the Shenzhen Key Laboratory of Ultrafast Laser Micro/Nano Manufacturing, Guangdong and Hong Kong Joint Research Centre for Optical Fibre Sensors, Shenzhen University, Shenzhen 518060, China (e-mail: hejia2019@email.szu.edu.cn; wujiafeng2021@email.szu.edu.cn; 2060453041@email.szu.edu.cn).

Fan Zhou, Benzhang Wang, and Yupeng Zhang are with the Innovation & Research Institute, Hiwing Technology Academy of CASIC, Beijing 100074, China (e-mail: 617754462@qq.com; wangbenzhang@hotmail.com; zhangyupeng209@163.com).

Color versions of one or more figures in this article are available at https://doi.org/10.1109/JLT.2024.3503579.

Digital Object Identifier 10.1109/JLT.2024.3503579

core-clad structures from rod-in tube source rods and hence has no protective coating or conventional cladding, resulting in multimode operation. Then the reflection spectra of sapphire fiber Bragg gratings (SFBGs) exhibit a large bandwidth of about 7 nm, which is much larger than that of conventional single-mode FBGs (e.g., 0.5 nm). By using complicated processes, such as spectra averaging, long-wavelength edge detection, and cross-correlation algorithm, the peak searching dispersion still only achieves ±10 pm, which seriously hampers the sensing accuracy [8], [9], [10]. It requires suppressing the high-order modes to solve this problem fundamentally, and then, two methods, i.e., the tapered fiber coupling and offset coupling, have been proposed [11], [12]. The bandwidth can be effectively reduced to 0.33 nm, resulting in a higher peak searching accuracy. However, these methods require precise alignment and are inconvenient for practical use.

A single-mode SFBG is considered to be the more feasible solution. The thermal acid etching method has been proposed to fabricate a single-mode micro-SFBG. The reflection spectrum exhibits discrete narrow-band peaks, but the mechanical strength decreases severely [13]. The ion-implanted method was demonstrated to create graded refractive index cladding, making the fiber's intensity profile nearly single mode. However, this method requires special equipment (i.e., neutron sources), which is expensive and not easily available [14]. In addition, the sapphire-derived fibers obtained by inserting the sapphire fiber into a silica tube and pulling it at high temperatures were proposed to achieve the single-mode sapphire fiber [15]. However, the silica cladding limits sensors operated below 1200 °C. To enhance the operation temperature, various cladding materials, such as polycrystalline Al_2O_3, metal Mo, ZrO_2, and SiBCN have been proposed [16]. Due to thermal instability and unmatchable refractive index, this method still has many challenges.

Femtosecond-laser-inscribed single-mode SFBG is a promising approach. Depressed cladding waveguide was created in sapphire materials successfully [17], and then the Bragg grating was inscribed in this waveguide, which generates the single mode Bragg resonance [18]. Whereafter, we proposed the single-step method for creating single-mode Bragg grating waveguides based on helical structure, which serves as a depressed cladding waveguide and also generates strong Bragg resonance due to its periodicity [19]. This indicates that a single-mode SFBG can be fabricated by using this method.

In this paper, we propose the creation of a single-mode helical Bragg grating waveguide (HBGW) in a sapphire fiber by using a femtosecond laser direct writing technique. However, the focal-point distortion induced by the cylindrical geometry of the fiber hampers the perfect inscription of the helical structure. We used a slit to solve this problem. An optimized spot-like inscription was achieved, and then regular ring patterns can be induced within the sapphire fiber. Moreover, three helical SFBGs with various diameters have been fabricated. The mode field characteristics and spectra were studied. The results show that a single-mode SFBG can be obtained by using the optimizing writing parameters (i.e., a diameter of 14 μm and a period of 1.78 μm). Such a device has a narrow bandwidth of 0.18 nm and a high reflectivity of 66.3%. In addition, the temperature responses
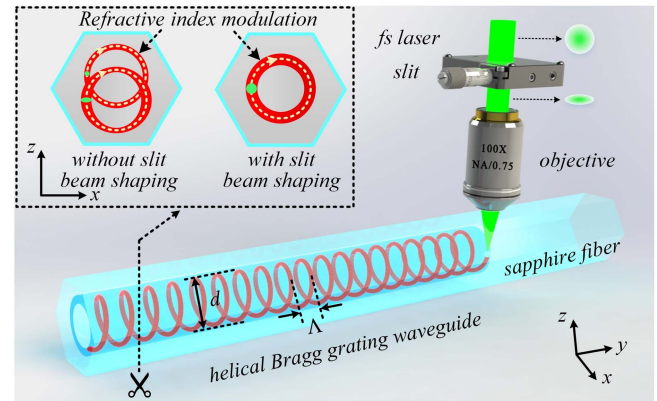

Fig. 1. Schematic of an HBGW created in sapphire fiber by using femtosecond laser direct-writing technique. Insets: schematic in cross-sectional view of the HBGW inscribed with slit and without slit.

of the HBGWs were also tested, exhibiting a temperature sensitivity of ~33.9 pm/°C at 1200 °C and good repeatability in temperature measurements.

II. Device Fabrication and Characterization

The experimental setup used for creation of the proposed HBGW into sapphire fibers are displayed in Fig. 1. A frequency-doubled regenerative amplified Yb:KGW [KGd(WO$_3$)] femtosecond laser (Pharos, Light Conversion) with a central wavelength of 514 nm, a pulse width of 290 fs, a repetition rate of 200 kHz and a laser spot diameter of 3 mm was employed as the laser source. A 100× Leica dry objective with a numerical aperture (N.A.) of 0.75 was selected as the focusing element, which can be used for inscription in a free-standing fiber without the need for oil immersion. But the distortion occurs due to the cylindrical geometry of the fiber. Hence, an adjustable mechanical slit (Thorlabs, VA100) was inserted in front of the objective, to alleviate such inscription distortion [20], [21]. Moreover, a commercial single-crystal sapphire fiber (Jingying Inc.) with a diameter of 100 μm was employed for fabricating HBGWs. An assembled three-axis air-bearing translation stage (Aerotech, ABL15010, ANT130LZS, and ANT130V-5), with the transverse and vertical resolution of 5 nm and 2 nm, respectively, was used to precisely translate the fiber.

The process for fabricating an HBGW in the sapphire fiber is also illustrated in Fig. 1. At first, the sapphire fiber with a length of 1 cm was spliced with two segments of single-mode fiber (SMF, Corning, G652D), which was mounted on the 3D translation stage with a pair of fiber holders. And then, the axial direction of the fiber was adjusted parallel to the translation along the y-axis. Subsequently, the shutter was opened, and the femtosecond laser beam was focused into the sapphire fiber. In this process, the sapphire fiber was translated in a helical trajectory via synchronous movements along the x, y, and z axes, and a helical structure was hence inscribed in the sapphire fiber. As shown in the inset of Fig. 1, when the helical structure was inscribed without slit beam shaping, its cross section is irregularly annular. By inserting the slit, this problem can be solved, and the perfect cross-section can be obtained, which
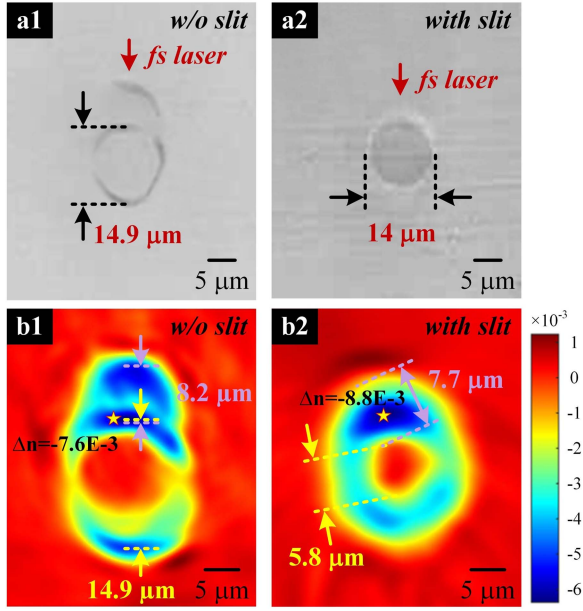
Fig. 2. The cross-sectional view of ring patterns inscribed without slit and with slit, (a1) and (a2) microscope images, (b1) and (b2) refractive index distribution.
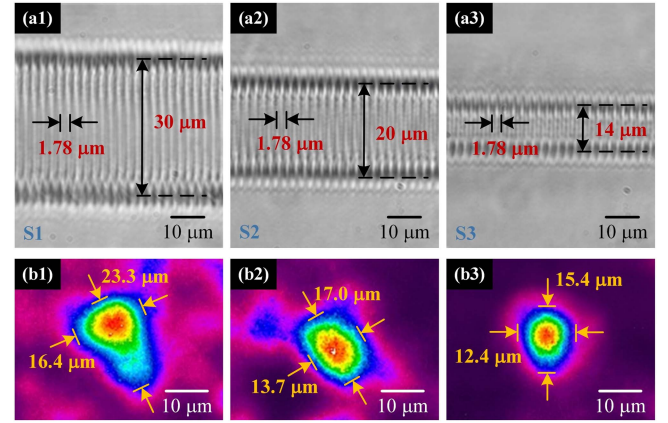

Fig. 3. Lateral view microscope images and transmission modes of three fabricated HBGW samples in sapphire fibers S1, S2 and S3 with decreasing diameters of 30, 20 and 14 μm, respectively. (a) Lateral view microscope images and (b) near-field profiles of transmission mode at the resonant wavelength of 1550.33 nm.

serves as a depressed cladding. Simultaneously, the helical trajectory provides a periodic structure, which can yield a Bragg grating resonance.

At first, we investigated the effect of the use of the slit on the shape of the inscription pattern. The ring pattern with a diameter of 14 μm was inscribed into the sapphire fiber without the slit. The writing parameters including pulse energy, repetition rate, and velocity are set as 21.7 nJ, 200 kHz and 0.5 mm/s, respectively. As shown in Fig. 2(a1), the inscription pattern is not a regular ring in the cross-section. And then the refractive index distribution was measured by using digital holographic microscopy (SHR-1602, index accuracy: 10^{-4}) produced by Shanghai University, China. As displayed in Fig. 2(b1), it could be found that the inscription pattern consists of two rings with an offset of 8.2 μm. Such an irregular structure can be not used to construct the HBGW. To solve this problem, we inserted a slit with an optimized width of 0.35 mm. The on-target energy was set as 21.7 nJ, and then a regular ring pattern with a diameter of 14 μm was inscribed, as shown in Fig. 2(a2) and (b2), which demonstrates that the focal-point distortion induced by the cylindrical geometry of the fiber was eliminated completely. As shown in Fig. 2(b1) and (b2), the negative refractive index change is formed by a micro-explosion for the case of high-energy femtosecond laser pulses, leading to the shock and rarefaction waves and resulting in a permanently damaged area [3], [22]. Moreover, the maximum negative refractive index change is -8.8 $\times$ 10^{-3}, and the width of the ring is $\sim$7.7 μm, ensuring the optical confinement in the HBGW [20].

Subsequently, we fabricated three HBGW samples in sapphire fibers, S1, S2, and S3, with decreasing helical diameters of 30, 20, and 14 μm using the optimizing writing parameters (i.e., slit width of 0.35 mm, on-target pulse energy of 21.7 nJ). All of

them have the same length of 1 cm. As shown in Fig. 3(a1)–(a3), periodic Bragg grating structures can be seen from the lateral view, the helical period of three samples was measured as 1.78 μm. The near-field profiles of transmission mode in HBGWs were measured by using a tunable laser (Keysight, 81940A, with central wavelength set to be 1550.33 nm) and a mode observation system consisting of lens and CCD (Newport, LBP2-HR-IR2). In the case of S1 (i.e., HBGW with a diameter of 30 μm), the multimode operation could be observed from the near-filed profile of the transmission mode illustrated in Fig. 3(b1). The mode field is an irregular pattern with diameters of 23.3 μm $\times$ 16.4 μm. Moreover, in the case of S2 (i.e., HBGW with a diameter of 20 μm), the diameters of the mode field pattern decrease to 17.0 μm $\times$ 13.7 μm obviously, higher-order modes could be suppressed partially. However, the single mode is still not realized. Then, in the case of S3 (i.e., HBGW with a diameter of 14 μm), a fundamental mode can be observed in Fig. 3(b3). The diameters are measured as 15.4 μm $\times$ 12.4 μm, which is slightly larger than that of the single-mode silica fiber (i.e., $\sim$10 μm).

III. HIGH TEMPERATURE CHARACTERISTICS

Furthermore, the spectral characteristics of three HBGW samples in sapphire fibers S1, S2, and S3, were investigated by using a tunable laser (Keysight, 81940A) and an optical power meter (Keysight, N7744A). The wavelength resolution has been set as 0.5 pm. At first, we measured the transmission spectra of these samples. Previously, a reference spectrum was measured and recorded by using a single-mode fiber connected to the light source and the power meter. Then, the reflection spectra of these samples were measured by using a single-mode fiber coupler (50:50). As shown in Fig. 4(a) and (b), the transmission spectrum of S1 (i.e., HBGW with a diameter of 30 μm) exhibits a dip with a long wavelength edge. The out-of-band insertion loss of S1 is $\sim$6.03 dB, due to the mode-field diameter mismatch between the SMF (i.e., $\sim$10.4 μm $\times$ 10.4 μm) and the S1 (i.e.,
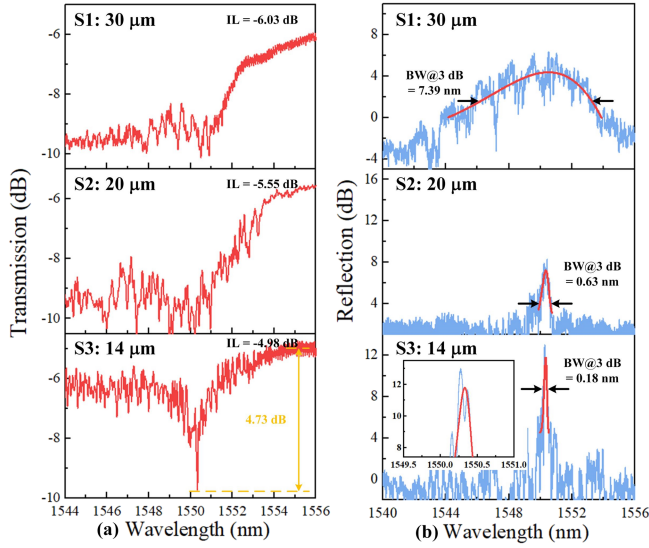
Fig. 4. Corresponding (a) transmission spectra and (b) reflection spectra of three fabricated HBGW samples in sapphire fibers S1, S2 and S3 with decreasing diameters of 30, 20 and 14 μm, respectively.
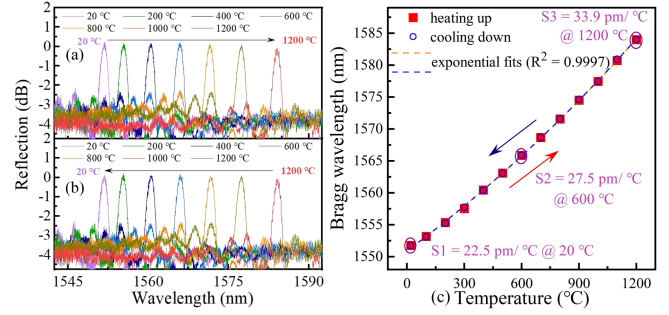

Fig. 5. Evolutions of reflection spectra of the single-mode SFBG during (a) the heating process and (b) the cooling process. (c) Bragg wavelengths of the single-mode SFBG as functions of the temperature in the case of temperature cycling from 20 °C to 1200 °C.

23.3 μm × 16.4 μm). Moreover, the reflection spectrum has a broad envelope. To obtain the bandwidth, the envelope was fitted by using a Gaussian-like curve, and then a 3-dB bandwidth was measured as 7.39 nm, which was consistent with the conventional multimode SFBGs [5], [6], [7]. These result from multimode operation in S1, which can be seen from the near-field profile of the transmission mode shown in Fig. 3(b1). In the case of S2 (i.e., HBGW with a diameter of 20 μm), the transmission spectrum still exhibits a dip with a long wavelength edge. Such a spectral shape is related to the strong coupling between the propagation modes with a continuum of radiation-like modes [23]. However, the out-of-band insertion loss of S2 is reduced to ~5.55 dB and the 3-dB bandwidth of the reflection envelope is reduced to 0.63 nm significantly, benefiting from the partial elimination of the higher-order modes, as shown in Fig. 3(b2).

In the case of S3 (i.e., HBGW with a diameter of 14 μm), the transmission spectrum exhibits a dip with an attenuation of 4.73 dB, rather than a sideband-like dip. This indicates that such an SFBG has a reflectivity of 66.3%. The 3-dB bandwidth of the reflection envelope is further reduced to 0.18 nm. As shown in the inset of Fig. 4(b), the reflection peak of S3 has obvious sidelobes, but its needle-like shape is similar to the Bragg grating inscribed in single-mode silica fiber. This results from the single-mode operation in S3, as shown in Fig. 3(b3). Additionally, an out-of-band insertion loss of ~4.98 dB can be observed in the transmission spectrum of S3, which mainly results from the mode-field diameter mismatch between the SMF (i.e., ~10.4 μm × 10.4 μm) and the S3 (i.e., 15.4 μm × 12.4 μm). This coupling loss could be reduced by further optimizing the diameters of the mode field.

Temperature response was tested by placing the single-mode SFBG into a tube furnace (Carbolite, Gero EST12/300) and monitoring the reflection spectrum evolution. The temperature in the furnace varied from 20 °C to 1200 °C and was maintained

for 30 min at each measurement point. Fig. 5(a) and (b) display the reflection spectra of the SFBG at various temperatures during the heating and cooling processes. In the test, the reflection peak has always maintained a stable Gaussian shape with a narrow bandwidth. Namely, a stubborn problem, i.e., deformation in the reflection spectrum of conventional multimode SFBG during high-temperature tests has been solved thoroughly. As displayed in Fig. 5(c), the complete high-temperature response of the single-mode SFBG from the room temperature up to 1200 °C. By using exponential fits to the measured data, the temperature sensitivity of the single-mode SFBG at various temperatures, that is 22.5 pm/°C at 20 °C, 27.5 pm/°C at 600 °C and 33.9 pm/°C at 1200 °C were evaluated. These results are consistent with the multimode SFBGs [5], [6], [7]. However, such a single-mode SFBG has much better repeatability than the previous multimode SFBGs, which thanks to its single-mode reflection peak with significant stability. Hence, such a single-mode SFBG is promising for the measurement of multiple physical parameters, such as high temperature, strain, pressure, and liquid level [1], [2], [24], [25]. Furthermore, it could be developed for the practical application of structural health monitoring in power plants, gas turbines, aerospace vehicles, and nuclear reactors.

IV. CONCLUSION

In this work, we have reported on the single-mode SFBG based on helical structure created by using a femtosecond laser direct writing technique. A slit was used to eliminate the focal-point distortion induced by the cylindrical geometry of the sapphire fiber. By using this method, a regular ring pattern with the maximum negative refractive index change of -8.8 × 10^{-3} and a width of 7.7 μm was inscribed within the sapphire fiber successfully, which can be used to create a depressed cladding waveguide. Moreover, after optimizing the writing parameters, a single-mode helical SFBG with a diameter of 14 μm and a period of 1.78 μm can be realized, exhibiting a narrow bandwidth of 0.18 nm and a high reflectivity of 66.3%. The temperature responses of single-mode SFBG were investigated, exhibiting increasing temperature sensitivity at elevated temperatures, i.e., 22.5 pm/°C at 20 °C, 27.5 pm/°C at 600 °C and 33.9 pm/°C at 1200 °C and a much better repeatability than the multimode

SFBGs. Therefore, such a single-mode SFBG can be applied for high-temperature measuring in many fields, such as power plants, gas turbines, and aviation.

REFERENCES

[1] S. Gao et al., "Review: Radiation temperature measurement methods for engine turbine blades and environment influence," *Infrared Phys. Technol.*, vol. 123, 2022, Art. no. 104204.

[2] A. Cavaliere and M. de Joannon, "Mild combustion," *Prog. Energy Combustion*, vol. 30, no. 4, pp. 329–366, 2004.

[3] J. He, B. J. Xu, X. Z. Xu, C. R. Liao, and Y. P. Wang, "Review of femtosecond-laser-inscribed fiber Bragg gratings: Fabrication technologies and sensing applications," *Photonic Sensors*, vol. 11, no. 2, pp. 203–226, 2021.

[4] P. Leonhard, D. Franz J., M. Robert R. J., B. Hartmut, and R. Johannes, "Regenerated Fibre Bragg gratings: A critical assessment of more than 20 years of investigations," *Opt. Laser Technol.*, vol. 134, 2021, Art. no. 106650.

[5] D. Grobnic, S. J. Mihailov, C. W. Smelser, and H. Ding, "Sapphire fiber Bragg grating sensor made using femtosecond laser radiation for ultrahigh temperature applications," *IEEE Photonic. Technol. Lett.*, vol. 16, no. 11, pp. 2505–2507, Nov. 2004.

[6] X. Z. Xu et al., "Sapphire fiber Bragg gratings inscribed with a femtosecond laser line-by-line scanning technique," *Opt. Lett.*, vol. 43, no. 19, pp. 4562–4565, 2018.

[7] T. Habisreuther, T. Elsmann, Z. W. Pan, A. Graf, R. Willsch, and M. A. Schmidt, "Sapphire fiber Bragg gratings for high temperature and dynamic temperature diagnostics," *Appl. Thermal Eng.*, vol. 91, pp. 860–865, 2015.

[8] T. Habisreuther, T. Elsmann, A. Graf, and M. A. Schmidt, "High-temperature strain sensing using sapphire fibers with inscribed first-order Bragg gratings," *IEEE Photon. J.*, vol. 8, no. 3, Jun. 2016, Art. no. 6802608.

[9] R. Eisermann et al., "Metrological characterization of a high-temperature hybrid sensor using thermal radiation and calibrated sapphire fiber Bragg grating for process monitoring in harsh environments," *Sensors*, vol. 22, no. 3, 2022, Art. no. 1034.

[10] X. Z. Xu et al., "Sapphire fiber Bragg gratings demodulated with cross correlation algorithm for long-term high-temperature measurement," *IEEE Sensors J.*, vol. 24, no. 6, pp. 7905–7911, Mar. 2024.

[11] D. Grobnic, S. J. Mihailov, H. Ding, F. Bilodeau, and C. W. Smelser, "Single and low order mode interrogation of a multimode sapphire fibre Bragg grating sensor with tapered fibres," *Meas. Sci. Technol.*, vol. 17, no. 5, pp. 980–984, 2006.

[12] X. Z. Xu, J. He, C. R. Liao, and Y. P. Wang, "Multi-layer, offset-coupled sapphire fiber Bragg gratings for high-temperature measurements," *Opt. Lett.*, vol. 44, no. 17, pp. 4211–4214, 2019.

[13] S. Yang, D. Homa, G. Pickrell, and A. B. Wang, "Fiber Bragg grating fabricated in micro-single-crystal sapphire fiber," *Opt. Lett.*, vol. 43, no. 1, pp. 62–65, 2018.

[14] B. A. Wilson and T. E. Blue, "Creation of an internal cladding in sapphire optical fiber using the ^{6}Li(n,α)^{3}H reaction," *IEEE Sensors J.*, vol. 17, no. 22, pp. 7433–7439, Nov. 2017.

[15] P. Dragic, T. Hawkins, P. Foy, S. Morris, and J. Ballato, "Sapphire-derived all-glass optical fibres," *Nat. Photon.*, vol. 6, no. 9, pp. 627–633, 2012.

[16] H. Chen, M. Buric, P. R. Ohodnicki, J. Nakano, B. Liu, and B. T. Chorpening, "Review and perspective: Sapphire optical fiber cladding development for harsh environment sensing," *Appl. Phys. Rev.*, vol. 5, no. 1, 2018, Art. no. 011102.

[17] J. P. Berube, J. Lapointe, A. Dupont, M. Bernier, and R. Vallee, "Femtosecond laser inscription of depressed cladding single-mode mid-infrared waveguides in sapphire," *Opt. Lett.*, vol. 44, no. 1, pp. 37–40, 2019.

[18] M. H. Wang et al., "Single-mode sapphire fiber Bragg grating," *Opt. Exp.*, vol. 30, no. 9, pp. 15482–15494, 2022.

[19] J. He et al., "Single-mode helical Bragg grating waveguide created in a multimode coreless fiber by femtosecond laser direct writing," *Photon. Res.*, vol. 9, no. 10, pp. 2052–2059, 2021.

[20] P. S. Salter, M. J. Woolley, S. M. Morris, M. J. Booth, and J. A. J. Fells, "Femtosecond fiber Bragg grating fabrication with adaptive optics aberration compensation," *Opt. Lett.*, vol. 43, no. 24, pp. 5993–5996, 2018.

[21] Y. J. Chen, Y. C. Lai, and M. W. Cheong, "Distortion-free femtosecond laser inscription in free-standing optical fiber," *Appl. Opt.*, vol. 55, no. 21, pp. 5575–5579, 2016.

[22] C. W. Smelser, S. J. Mihailov, and D. Grobnic, "Formation of type I-IR and type II-IR gratings with an ultrafast IR laser and a phase mask," *Opt. Exp.*, vol. 13, no. 14, pp. 5377–5386, 2005.

[23] J. R. Grenier, L. A. Fernandes, and P. R. Herman, "Femtosecond laser writing of optical edge filters in fused silica optical waveguides," *Opt. Exp.*, vol. 21, no. 4, pp. 4493–4502, 2013.

[24] A. Leal-Junior, A. Frizera, and C. Marques, "A fiber Bragg gratings pair embedded in a polyurethane diaphragm: Towards a temperature-insensitive pressure sensor," *Opt. Laser Technol.*, vol. 131, 2020, Art. no. 106440.

[25] A. G. Leal-Junior, C. Marques, A. Frizera, and Maria José Pontes, "Multi-interface level in oil tanks and applications of optical fiber sensors," *Opt. Fiber Technol.*, vol. 40, pp. 82–92, 2018.

Xizhen Xu was born in Guangdong, China, in 1990. He received the B.S. degree from the College of Science, Zhejiang University of Technology, Hangzhou, China, in 2013, and the M.S. and Ph.D. degrees in optical engineering from Shenzhen University, Shenzhen, China, in 2016 and 2019, respectively. From 2019 to 2021, he was with Shenzhen University, Shenzhen, China, as a Postdoctoral Research Fellow. He is currently with Shenzhen University, Shenzhen, China, as an Assistant Professor. He has authored or coauthored six patent applications and more than 70 journal and conference papers. His research interests include femtosecond laser micromachining, optical fiber sensors, and fiber Bragg gratings.

Jia He was born in Hunan, China, in 1997. She received the B.Eng. degree from the College of Physics and Optoelectronic Engineering, Xiangtan University, Xiangtan, China, in 2019, and the Ph.D. degree from the College of Physics and Optoelectronic Engineering, Shenzhen University, Shenzhen, China, in 2024. She is currently with Shenzhen University as a Postdoctoral Research Fellow. Her research interests include optical fiber sensors and fiber Bragg gratings.

Jiafeng Wu was born in Guangdong, China, in 1998. He received the B.S. degree from the College of Physics and Optoelectronic Engineering, Shenzhen University, Shenzhen, China, in 2021. He is currently working toward the Ph.D. degree with Shenzhen University. His research interests include fiber Bragg gratings and optical fiber sensors.

Runxiao Chen was born in Guangdong, China, in 1998. He received the B.S. degree from the College of Physics and Optoelectronic Engineering, Shenzhen University, Shenzhen, China, in 2020. He is currently working toward the Ph.D. degree with Shenzhen University. His research interests include femtosecond laser micromachining, fiber lasers, and optical fiber sensors.

Fan Zhou, biography not available at the time of publication.

Benzhang Wang, biography not available at the time of publication.

Yupeng Zhang, biography not available at the time of publication.

Yiping Wang (Senior Member, IEEE) was born in Chongqing, China, in 1971. He received the B.Eng. degree in precision instrument engineering from the Xi'an Institute of Technology, Xi'an, China, in 1995 and the M.S. and Ph.D. degrees in optical engineering from Chongqing University, Chongqing, in 2000 and 2003, respectively. From 2003 to 2005, he was with Shanghai Jiao Tong University, Shanghai, China, as a Postdoctoral Fellow. From 2005 to 2007, he was with the Hong Kong Polytechnic University, Hong Kong, as a Postdoctoral Fellow. From 2007 to 2009, he was with the Institute of Photonic Technology, Jena, Germany, as a Humboldt Research Fellow. From 2009 to 2011, he was with the Optoelectronics Research Centre, University of Southampton, Southampton, U.K., as a Marie Curie Fellow. Since 2012, he has been with Shenzhen University, Shenzhen, China, as a Distinguished Professor. He has authored or coauthored one book, 53 invention patents, and more than 420 journal and conference papers. His research interests include optical fiber sensors, fiber gratings, and photonic crystal fibers. Prof. Wang is the Fellow of Optica and the Chinese Optical Society.

Jun He (Member, IEEE) was born in Hubei, China, in 1985. He received the B.Eng. degree in electronic science and technology from Wuhan University, Wuhan, China, in 2006 and the Ph.D. degree in electrical engineering from the Institute of Semiconductors, Chinese Academy of Sciences, Beijing, China, in 2011. From 2011 to 2013, he was with Huawei Technologies, Shenzhen, China, as a Research Engineer. From 2013 to 2015, he was with Shenzhen University, Shenzhen, as a Postdoctoral Research Fellow. From 2015 to 2016, he was with The University of New South Wales, Sydney, NSW, Australia, as a Visiting Fellow. Since 2017, he has been with Shenzhen University, Shenzhen, China, as an Assistant Professor/ Associate Professor/ Distinguished Professor. He has authored or coauthored 15 invention patents and more than 125 journal and conference papers. His research interests include optical fiber sensors, fiber Bragg gratings (FBGs), and fiber lasers. Prof. He is a member of the Optical Society of America.